Journal of Alloys and Compounds 503 (2010) 266–271

Contents lists available at ScienceDirect

Journal of Alloys and Compounds

journal homepage: www.elsevier.com/locate/jallcom

Acetone mediated electrophoretic deposition of nanocrystalline SDC on NiO-SDC ceramics

A.G. Bhosale[a,b], Rajeev Joshi[b,e], K.M. Subhedar[c], R. Mishra[d], S.H. Pawar[b,e,*]

[a] Smt. Kusumtai Rajarambapu Patil Kanya Mahavidyalaya, Islampur 415409, Maharashtra, India
[b] Department of Physics, Shivaji University, Kolhapur 416 004, Maharashtra, India
[c] Department of Electrical Engineering, The Technion - Israel Institute of Technology, Haifa 32000, Israel
[d] Chemistry Division, Bhabha Atomic Research Centre, Mumbai 400085, Maharashtra, India
[e] Department of Technology, D.Y Patil University, Kolhapur 416006, Maharashtra, India

ARTICLE INFO

Article history:
Received 3 January 2010
Received in revised form 1 May 2010
Accepted 3 May 2010
Available online 9 May 2010

Keywords:
Ceramic
Thin film
Nanofabrications
Electronic properties
Scanning electron microscopy

ABSTRACT

Films of $Ce_{0.8}Sm_{0.2}O_{1.9}$ (SDC) were electrophoretically deposited on non-conducting NiO-SDC ceramics using the suspension of nanocrystalline SDC in acetone. The effect of iodine addition on suspension stability was investigated by measuring the zeta potential of SDC particle and pH of the suspension. The highest zeta potential was 42.1 mV with the addition of 2 mg iodine at pH 5.7 indicating formation of relatively stable suspension. The particle size distribution reveals the agglomerate size of SDC in acetone with iodine addition was of the order of 222 nm. The surface morphology and sintering effect on grain growth of the deposited films were investigated by scanning electron microscope (SEM). The structural investigation of the sintered film was done by X-ray diffraction (XRD) technique and it revealed phase pure SDC with cubic structure. Impedance study of sintered SDC/NiO-SDC hetero-structure showed decrease in total resistance with increase in temperature.

1. Introduction

One of the main challenges in today's solid oxide fuel cell (SOFC) technology is the reduction of their operating temperature. Thus new types of oxygen ion conducting materials are currently under investigation to overcome the problems which SOFC faces at high temperatures. Among ceria based solid electrolytes, $Ce_{0.8}Sm_{0.2}O_{1.8}$ (SDC) electrolyte has highest ionic conductivity as well as highest stability against reduction, commonly used for the application in intermediate solid oxide fuel cells (IT-SOFCs) [1–6]. The ionic conductors in thin film electrolyte form are of great interest for IT-SOFCs [7–10] due to ohmic loss of the electrolyte and its performance was found to increase in thin film form [11–13]. To reduce the cost of fabrication of SOFCs, formation of thin electrolyte film on electrode substrate is important. A suitable anode for SDC based SOFCs is generally suggested to be Ni-SDC ceramic, because of good electrochemical activity to oxidize fuels, high electronic conductivity, proper porosity at the micro-structural level and thermal compatibility with other components of the cell [7,14,15].

Recently, electrophoretic deposition (EPD) is gaining more interest as a ceramic processing technique for variety of technical applications like ceramic composites, electrodes and coating for electronics, catalytic and electrochemical applications [16].

Electrophoretic deposition is a colloidal deposition process and it easily controlled by applied electric field. The EPD is especially attractive in solid oxide fuel cells (SOFCs) fabrication due to its simple, low cost equipment and ease of deposition of films of controlled thickness even on substrates with complex shapes. Therefore, EPD is expected to be the best alternative for preparation of thin film electrolytes with size-controlled particles, which are highly desirable for fuel cell to operate at reduced temperature with higher efficiency [17,18]. The mechanism of EPD involves deposition of charged particles in the suspension on to an electrode under the influence of applied electric field. Different parameters considered for characterizing the nature of suspension are physiochemical behavior of both suspended particles and liquid medium, surface properties of the particle and influence of concentration of additives. For achieving best EPD process, these parameters are to be well understood and optimized. The EPD of YSZ solid electrolyte is extensively studied in the literature [19–22]. But detailed studies of different EPD parameters for stable suspension of SDC powder on ceramic substrates are few to date. In the present work, synthesis of SDC thin film on NiO-SDC substrates in acetone medium by EPD and their characterization has been reported. The work is in continuation with our earlier report of SDC film formation on stainless steel substrate [23]. Acetone medium is chosen for the formation of SDC colloidal suspension due to low viscosity and

* Corresponding author at: Centre For Interdisciplinary Research, D.Y. Patil University, Kolhapur 416006, M.S., India.
E-mail address: pawar_s_h@yahoo.com (S.H. Pawar).

0925-8388/$ – see front matter © 2010 Elsevier B.V. All rights reserved.
doi:10.1016/j.jallcom.2010.05.013

considerable dielectric constant, since it is useful for intermediate applied voltage for EPD on ceramic substrates [24]. The suspension media should not be too volatile in order to prevent formation of pores and cracks during shrinkage of deposit. The EPD parameters such as zeta potential, particle size distribution in acetone medium with and without addition of iodine and corresponding pH values of the suspension is studied in detail. The optimal content of solid iodine for well-dispersed suspension is determined from zeta potential measurement. Effect of sintering on grain growth of electrophoretically deposited film is studied. The electrical property of the formed hetero-structure is determined from impedance measurement in the temperature range of 473–791 K.

2. Experimental details

2.1. Materials and substrate preparation

The nanocrystalline SDC and NiO powders used for electrophoretic deposition and in anode preparation respectively were synthesized by solution combustion method using polyvinyl alcohol (PVA) as a fuel [25]. The starting materials were Sm_2O_3 (purity ~99.99%), Ce $(NO_3)_2{\cdot}6H_2O$ (purity 99.95%), Ni $(NO_3)_2$ (purity ~99.99%), PVA $(-C_2H_4O)_n$ from Loba chemicals, India. The detailed synthesis of SDC nanopowder is reported elsewhere [23]. Acetone (electronic grade, 99.99% pure) as solvent and solid iodine as an additive were used for the preparation of SDC suspension.

The substrates used for electrophoretic deposition of SDC were prepared by mixing the composition of NiO and SDC powder in the ratio of 75:25 wt% with addition of PVA binder [26]. The nanocrystalline powders of NiO and SDC with PVA binder were mixed using agate mortar and pestle up to 8 h. The homogenized mixer was isostatically pressed into the pellets under the pressure of 10 tons up to 5 min having dimensions of ~1.4 cm diameter and 0.15 cm thickness. The pellets were sintered at about 1273 K for 4 h to burn off the binder leaving behind porous substrate. The porosity of the sintered pellets was close to ~34% as measured by Archimedes method using water.

2.2. Suspension preparation

The first step in EPD is to prepare a stable suspension of ceramic particles in a solvent suitable for development of adequate surface charge on the particles in order to enhance deposition rate and produce uniform and homogeneous deposition. The stable suspension of SDC was prepared by dispersing known weight of powder in a solvent with addition of iodine as an additive. The suspension bath was sonicated in a high intensity ultrasonic bath, in order to deagglomerate the particles and it was equilibrated up to 6 h and again sonicated before EPD.

In EPD, addition of solid iodine in acetone bath is responsible for charging the particle surface and it found to be best in terms of stability of suspension and deposition quality [27]. The SDC particles in acetone bath added with solid iodine acquire positive charge and it migrates towards an oppositely charged electrode during the EPD. The optimized concentration of SDC in acetone was 30 mg/30 ml, confirmed by optical method. The detailed experiment is reported in our earlier work [23].

Zeta potential and corresponding pH values of the suspension were measured by using Zetasizer (Malvern Instruments Ltd.) and pH meter (waterproof pH scan-2, Eutech Instrument), respectively. The optimal content of iodine in the suspension corresponding to maximum zeta potential was used in EPD experiments. The particle size distribution of SDC nanocrystallites in acetone medium with and without addition of iodine was analyzed by CONTIN method using dynamic light scattering (DLS) technique. The chemical character of SDC solid surface in acetone was also investigated by changing the pH level of the solution with addition of 0.1 mM of HCl and NaOH solution.

2.3. Deposition procedure

The experimental set up used in EPD consists of two electrodes of stainless steel fixed in a holder made up of bakelite. A graphite circular disc of diameter 1.5 cm and 0.1 mm thickness was fixed on a stainless steel electrode. The NiO-SDC porous substrate was mounted on a graphite disc and it acts as deposition electrode. Distance between the deposition and counter electrode was kept constant at about 0.5 cm. The area of electrode exposed for deposition in EPD bath was maintained constant at 2.25 cm^2. The EPD experiments were carried out at room temperature under constant D.C. voltage of 100 V using high voltage D.C. power supply unit (Aplab high voltage D.C. power supply, H1003) with deposition time 7 min.

2.4. Characterization of film

The deposited SDC films on ceramic substrate were sintered at 1423 K and 1523 K for 6 h, respectively and 1623 K for 12 h. They were named as sample 1, 2 and 3, respectively. The morphology of the as-deposited film and effect of sintering on grain growth of the deposited films on the substrate were investigated by scanning electron microscope (SEM, model JEOL JSM 6360). The XRD pattern of sample 3 was recorded by X-ray diffractometer (Philips-3710), with Cu Kα radiation (λ = 1.5418 Å) in the 2θ range from 20° to 80°. The patterns were evaluated by X' pert high score software and compared with JCPDS data (card no.75-0158). For impedance measurement, platinum paste was painted on the opposite faces of sample 3. The sample was dried and then heated in an electric oven at 473 K up to 6 h before the measurements to ensure good bonding. A.C. conductivity measurements were carried out in air by parallel plate capacitor geometry with an applied r.m.s. voltage of 100 mV (Solatron 1260, frequency response analyzer) at frequencies ranging from 1 Hz to 1 MHz over temperature range 473–791 K.

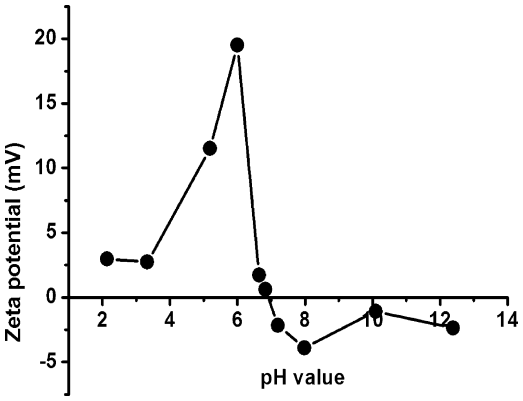

Fig. 1. Variation of the zeta potential of SDC nanocrystallite with different pH level of the suspension by addition of 0.1 mM HCl and NaOH solution.

3. Results and discussion

3.1. Chemical behavior of SDC nanoparticles

The chemical nature of the ceramic solid surface can be understood by inducing surface charge on ceramic particles by the addition of acid or base [21]. Recording the corresponding pH and zeta potential can provides a valuable guideline for the suspension preparation. Zeta potential measurements only give an indication about the nature of surface charge and potential which are adequate for stability of the suspension. It measures the potential difference between the particle surface and shear layer plane formed by the adsorbed ions.

Herein, the nanocrystalline SDC powder is suspended in acetone bath and the pH level of the suspension was modulated from acidic to alkaline by addition of 0.1 mM HCl (pH < 7) and 0.1 mM of NaOH (pH > 7), respectively. Fig. 1 demonstrates the zeta potential variation of SDC nanocrystallites at different pH levels of the suspension. It revealed that, with addition of alkali to the suspension bath, SDC particles tend to acquire negative charge due to OH^- capsulation and it results in negative zeta potential. On the other hand, with addition of acid to the suspension, SDC particle surface acquires a neutral charge for pH 7. Further addition of acid causes a build-up of positive charge due to adsorption of H^+ ions on solid surface and it acquires positive zeta potential. Thus, variation of zeta potential with pH level shows positive zeta potential at acidic pH and it is highest for pH 6. The zeta potential is negative at basic pH and it is found to be less. The plot passes through zero zeta potential known as isoelectric point (IEP) for pH 7, where the agglomeration is more likely to occur and colloidal system becomes unstable [28].

3.2. Effect of iodine addition on pH and zeta potential

The variation of zeta potential depends on many factors such as steric effect between particle surface and the concentration of additives and type of ions in the solution etc. [28]. The absolute value of zeta potential should be high in order to create a stable colloidal dispersion. Commonly ±30 mV is accepted as the threshold for sta-

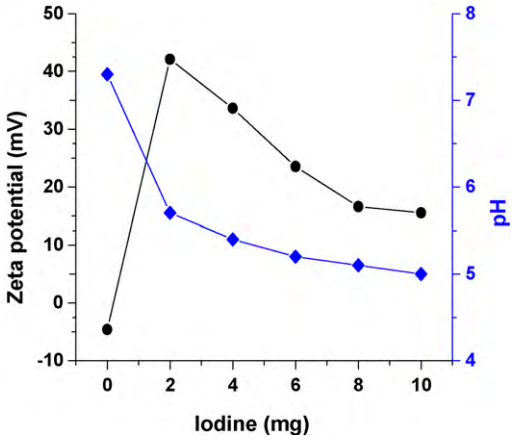

Fig. 2. Variation of zeta potential with addition of solid iodine content (mg) and pH.

bility in many colloidal systems. It is reported that, an appropriate addition of iodine in the suspension bath enhances concentration of H^+, hence the pH. These H^+ ions get adsorbed on the surface of particles in the suspension [29].

Fig. 2 shows the effect of iodine addition on pH of the suspension and corresponding zeta potential of SDC particle. It revealed that, without addition of iodine in the suspension, zeta potential is negative for pH 7.3 and it is nearer to the isoelectric point as seen from Fig. 1. Thus, it predicted that suspension with lower negative zeta potential is more unstable. As iodine concentration increases from 2 mg to 10 mg, the concentration of the H^+ ions in the suspension increases and hence pH of the suspension decreases from 5.7 to 5. The reaction between acetone and iodine is expected to release H^+ ions according to following reaction [30],

$$CH_3–CO–CH_3 + 2I_2 \leftrightarrow ICH_2–CO–CH_2I + 2H^+ + 2I^- \quad (I)$$

As iodine content in the suspension increases, the positive zeta potential of the SDC particle decreases and then remains nearly same at higher concentration. The maximum zeta potential is found to be 42.1 mV for 2 mg of iodine of pH 5.7. This is attributed due to the fact that, adsorption of H^+ ions onto the particle surface which enhances strong electrostatic repulsive force, that prevents the particle agglomeration and thus it increases the stability of the suspension. At higher content of iodine, the pH of the suspension is not much affected. This is due to increased adsorption of H^+ ion on particle surface which saturates and corresponding zeta potential becomes lower. This is because of reduction of double layer thickness; which will decrease the repulsive force between the particles. Thus, due to existence of much weaker and potentially reversible adhesion between the particles, zeta potential reduces at higher concentration of iodine.

3.3. Effect of iodine addition on pH and particle size distribution

Fig. 3a and b shows the particle size distribution of SDC nanocrystallites in acetone with and without addition of iodine. Before addition of iodine, the size distribution peak of SDC revealed two different agglomerate distributions. According to Derjaguin, Landu, Verway and Overbeck (DLVO) theory [31], the main reason for agglomeration in the suspension is electrostatic attractive force, which is larger than repulsive force from double layer between the particles. The average agglomerate size of SDC without iodine was found to be 692 nm for pH 7.3 and corresponding zeta potential observed from Fig. 2 is −4.82 mV. Thus, it confirmed that for lower negative zeta potential at pH 7.3, the electrostatic repulsive force is not strong enough to overcome the attractive van der Waal force between the particles, causing destruction of colloidal stability.

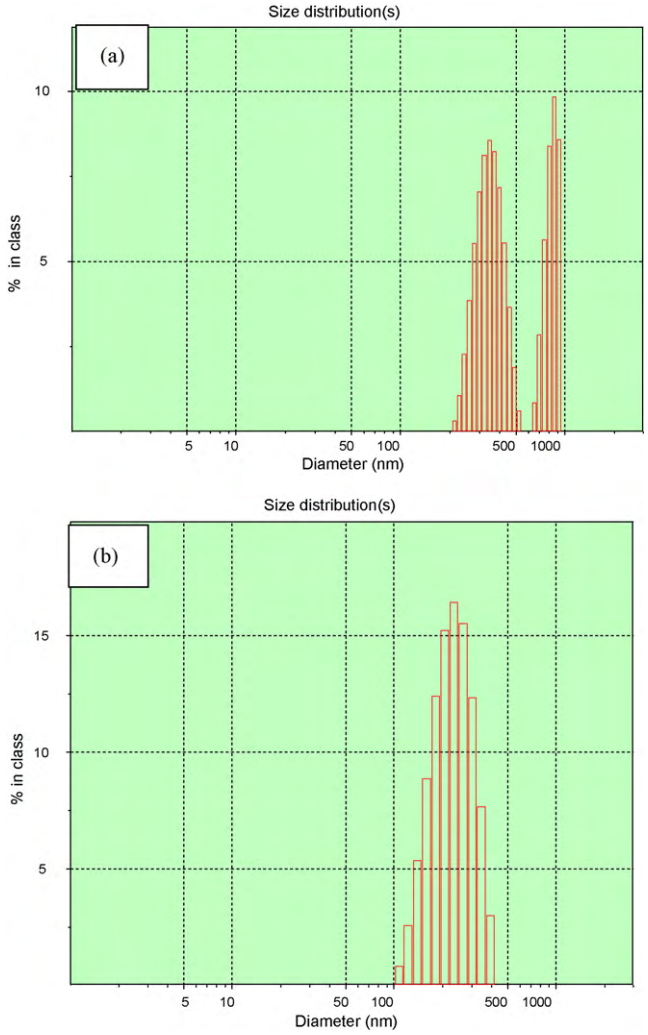

Fig. 3. Particle size distribution of SDC nanocrystallites (a) without iodine and (b) with iodine.

Fig. 3b shows single size distribution peak for addition of 2 mg iodine in the suspension and it revealed the agglomerate size of SDC to be 222 nm at pH 5.7, with maximum zeta potential. Thus, addition of small content of iodine in the suspension reduces the pH and helps to reduce the agglomerate size of SDC; it is least at pH 5.7 with highest zeta potential suitable for stable suspension.

3.4. Characterization of films

Fig. 4a and b shows surface and cross-sectional SEM of the as-deposited film on NiO-SDC substrate prepared from 30 mg/30 ml solid loaded acetone-based suspension added with 2 mg iodine under constant applied potential of 100 V for 7 min. Fig. 4a depicts that the film formation is smooth and uniform. The thickness of as-deposited film shown in Fig. 4b is found to be more than 10 μm. Further for well adherence of film with substrate and improving packing density of particles, the samples are sintered at different temperature with different sintering time. Fig. 5a–c shows the effect of sintering temperature on the resulting grain growth of electrophoretically deposited SDC films of sample 1, 2 and 3, respectively. It revealed that as sintering temperature increased, the microstructure of the deposited films is modified significantly. The sample 3 sintered at 1623 K for prolonged time (12 h) is found to form well-compact film surface with good grain connectivity suitable for electrolyte material.

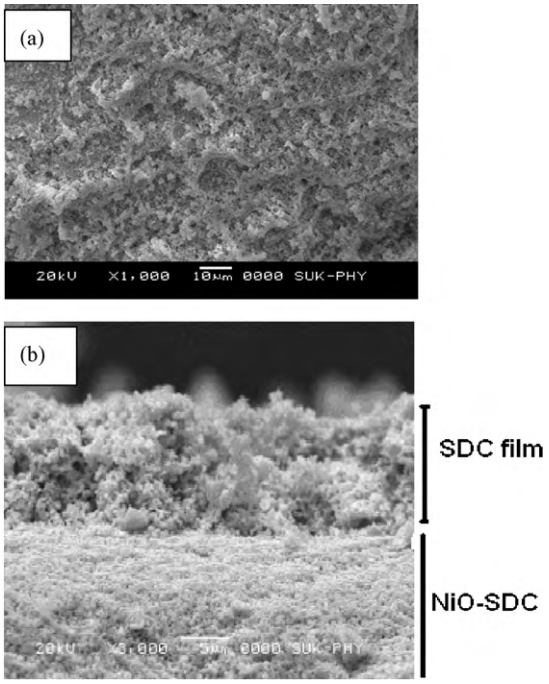

Fig. 4. (a) Surface morphology and, (b) cross-sectional view of as-deposited SDC thin film on NiO-SDC substrate.

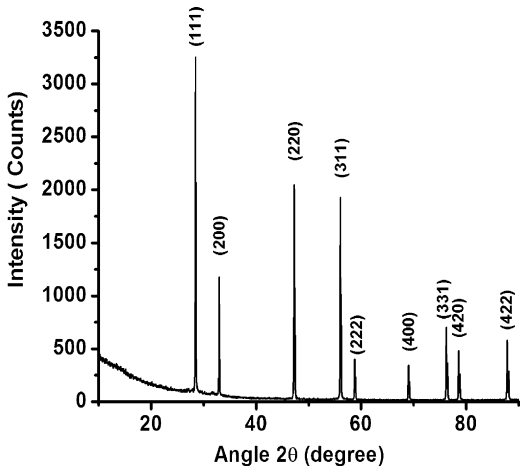

Fig. 6. XRD pattern of the SDC/NiO-SDC hetero-structure sintered at 1623 K for 12 h.

Fig. 6 shows XRD pattern of SDC film on NiO-SDC, sintered at 1623 K for 12 h (sample 3). The reflection peaks observed in Fig. 6 are labeled according to the JCPDS file (card no.75-0158), which confirmed the phase pure SDC film with cubic structure. The crystallite size is calculated by using Debye–Scherrer formula as:

$$D = \frac{0.9\lambda}{\beta \cos\theta_B} \quad (1)$$

where D – crystallite size in nm, λ – incident X-ray wavelength in Å, β – full width at half maxima (FWHM) in radian corresponding to maximum intensity (angular width in 2θ) and θ_B is Bragg angle. The crystallite size of SDC, of samples 1 and 3 using Eq. (1) are found to be 43 nm and 70 nm, respectively. The increased crystallite size of SDC is attributed due to granular structure of the film at higher temperature for prolonged sintering time compared to other samples.

A.C. impedance methods are widely used for investigating the electrical behavior of the material over wide range of frequency

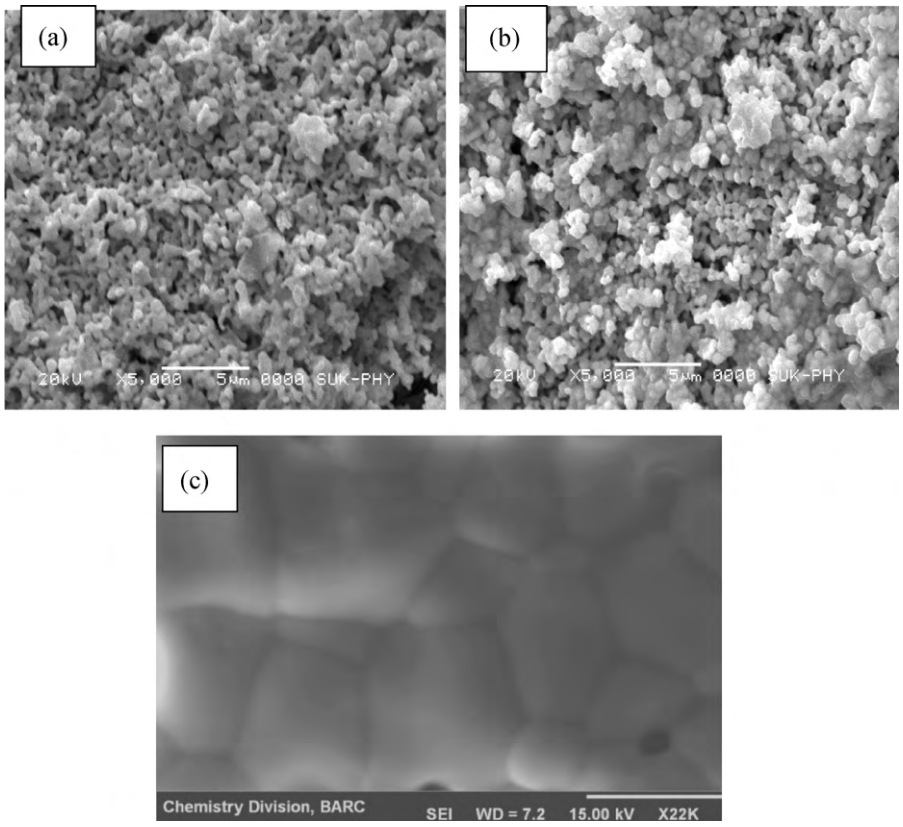

Fig. 5. Surface morphology of SDC thin film on NiO-SDC substrate sintered at, (a) 1423 K for 6 h, (b) 1523 K for 6 h (c) 1623 K for 12 h.

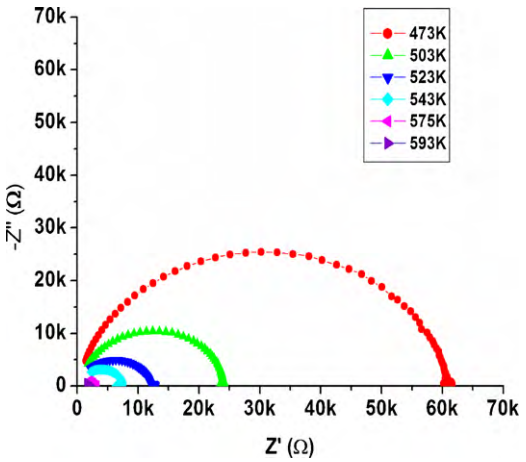

Fig. 7. Cole–Cole plot for SDC/NiO-SDC hetero-structure sintered at 1623 K for 12 h in the temperature range of 473–593 K.

and temperature, which helps to separate the real and imaginary components of the electrical parameters and hence provide a better understanding of material properties. Fig. 7 shows complex impedance spectrum i.e. Cole–Cole plots of sample 3 under investigation, measured at different temperatures ranging from 473 K to 593 K. The intercept of each semicircle arc with real axis Z' gives bulk resistance of the half-cell formed by SDC coating on NiO-SDC substrate and it decreases with increase in temperature.

The bulk conductivity was found to follow Arrhenius nature given by:

$$\sigma = \frac{\sigma_o}{T} \exp\left(\frac{-E_a}{KT}\right) \quad (2)$$

where E_a – activation energy for conduction, T – absolute temperature, K – the Boltzmann constant and σ_o – pre-exponential factor.

The typical plot of $\ln(\sigma T)$ vs. $1000/T$ for sample 3 is shown in Fig. 8. The total resistance of the half-cell drops drastically above 593 K. Fig. 9 shows the reduction in half-cell resistance for the temperature range 725–791 K. It revealed that as, temperature increases, the electrode resistance (which is the resistance on real axis from origin to the high frequency impedance intercept) also decreases. The response shifts towards origin with increasing temperature drastically. This indicates that the on-set temperature for cell operation pins above 593 K. This on-set temperature is less than the earlier reported value for the same hetero-structure [32].

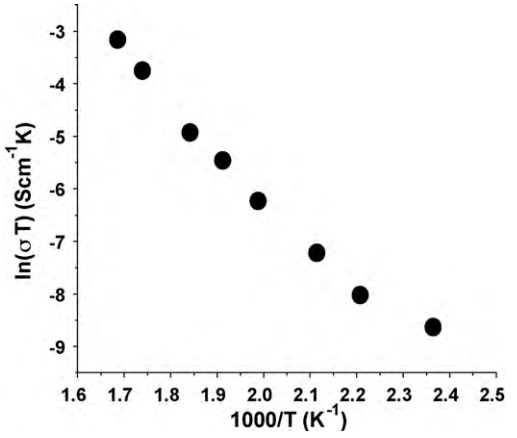

Fig. 8. Arrhenius plot for SDC/NiO-SDC hetero-structure sintered at 1623 K for 12 h in the temperature range of 473–593 K.

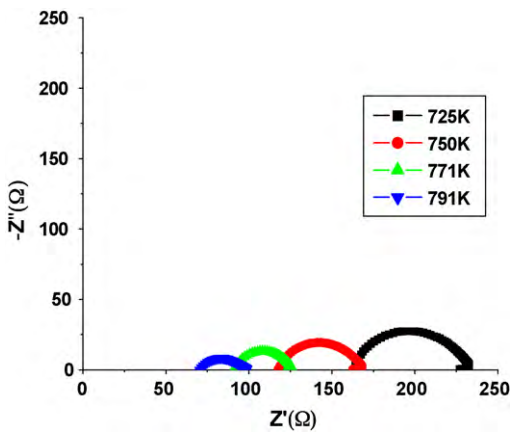

Fig. 9. Cole–Cole plot for SDC/NiO-SDC hetero-structure sintered at 1623 K for 12 h in the temperature range of 725–791 K.

4. Conclusions

The electrophoretic deposition technique is shown to be an easy and cost-effective method for the production of densely grained SDC film on circular shaped non-conducting porous NiO-SDC substrates. The study showed that acetone with iodine additive could effectively form relatively stable and well-dispersed SDC colloidal suspension suitable for EPD. The zeta potential of SDC particle in acetone was found to be optimum for 2 mg iodine for pH 5.7 and corresponding agglomerate size obtained from analysis of particle size distribution is 222 nm. The sintering of the hetero-structure at temperature about 1623 K for 12 h improved the grain structure of SDC film. Impedance studies showed that the bulk resistance of the half-cell decreases with increase in temperature and has lesser bulk resistance at higher temperature.

Acknowledgements

Authors are thankful to Dr. C.A. Betty, Scientist BARC Mumbai for useful discussions. One of the authors A.G. Bhosale would like to thank the Principal, Kusumtai Rajarambapu Patil Kanya Mahavidyalaya, Islampur and management committee of Kasegaon education society for their encouragement and motivation for this work.

References

[1] S. Hui, J. Roller, S. Yick, X. Zhang, C. Decès-Petit, Y. Xie, R. Maric, D. Ghosh, J. Power Sources 172 (2007) 493.
[2] H. Inaba, H. Tagawa, Solid State Ionics 83 (1996) 1.
[3] K. Eguchi, J. Alloys Compd. 20 (1997) 486.
[4] Y.-P. Fu, S.-H. Chen, J.-J. Huang, Int. J. Hydrogen Energy 35 (2010) 745.
[5] W.-C. Wu, J.-T. Huang, A. Chiba, J. Power Sources 195 (2010) 5868.
[6] E.C.C. Souza, H.F. Brito, E.N.S. Muccillo, J. Alloys Compd. 491 (2010) 460.
[7] I. Taniguchi, T. Hosokawa, J. Alloys Compd. 460 (2008) 464.
[8] G. Laukaitis, M. Jauneika, J. Dudonis, O. Katkauske, D. Milcius, Vacuum 83 (2009) S114.
[9] G. Laukaitis, J. Dudonis, D. Virbukas, Surf. Coat. Technol. 204 (2010) 2028.
[10] H. Shi, W. Zhou, R. Ran, Z. Shao, J. Power Sources 195 (2010) 393.
[11] R.S. Joshi, R.K. Nimat, S.H. Pawar, J. Alloys Compd. 466 (2008) 341.
[12] R.K. Nimat, R.S. Joshi, S.H. Pawar, Mater. Sci. Eng. B 137 (2007) 93.
[13] R.S. Joshi, R.K. Nimat, S.H. Pawar, J. Alloys Compd. 471 (2009) 461.
[14] X. Fang, G. Zhu, C. Xia, X. Liu, G. Meng, Solid State Ionics 168 (2004) 31.
[15] C. Xia, F. Chen, M. Liu, Electrochem. Solid-State Lett. 4 (2001) A52.
[16] A.R. Boccaccini, I. Zhitomirsky, Curr. Opin. Solid State Mater. Sci. 6 (2002) 251.
[17] T. Hosomi, M. Matsuda, M. Miyake, J. Eur. Ceram. Soc. 27 (2007) 173.
[18] L. Jia, Z. Lu, X. Kuang, Z. liu, K. Chen, X. Sha, G. Li, W. Su, J. Alloys Compd. 424 (2006) 299.
[19] H. Xu, Ian P. Shapiro, P. Xiao, J. Eur. Ceram. Soc. 30 (2010) 1105.
[20] S.T. Aruna, K.S. Rajam, Mater. Chem. Phys. 111 (2008) 131.
[21] L. Besra, C. Compson, M. Liu, J. Power Sources 173 (2007) 130.
[22] P. Garcia, B. Ferrari, R. Moreno, A.J. Sánchez-Herencia, M.T. Colomer, J. Eur. Ceram. Soc. 27 (2007) 4241.

[23] A.G. Bhosale, M.B. Kadam, Rajeev Joshi, S.S. Pawar, S.H. Pawar, J. Alloys Compd. 484 (2009) 795.
[24] H. Negishi, N. Sakai, K. Yamaji, T. Horita, Y. Yokokawa, J. Electrochem. Soc. 147 (2000) 1682.
[25] J. Ma, C. Jiang, X. Zhou, G. Meng, X. Liu, J. Power Sources 162 (2006) 1082.
[26] S. Wang, M. Ando, T. Ishihara, Y. Takita, Solid State Ionics 174 (2004) 49.
[27] R.S. Hyam, K.M. Subhedar, S.H. Pawar, Colloids Surf. A 297 (2007) 172.
[28] R. Xu, Particle Characterization: Light Scattering Method, 1st ed., Kluwer Academic Publishers, The New York, 2000, p.294.
[29] N. Koura, T. Tsukamoto, H. Shoji, T. Horita, Jpn. J. Appl. Phys. 34 (1995) 1643.
[30] T. Mathews, N. Rabu, J.R. Sellar, B.C. Muddle, Solid State Ionics 128 (2000) 111.
[31] L. Besra, M. Liu, Prog. Mater. Sci. 52 (2007) 1.
[32] S. Nakayama, M. Miyayama, Eng. Mater. 350 (2007) 175.